Journal of the European Ceramic Society **13** (1994) 461–465

Preparation of R–α'–β'-Sialons (R = Sm, Gd, Dy, Y and Yb) by Pressureless Sintering

Hao Wang, Wei-Ying Sun, Han-Rui Zhuang & Tung-Sheng Yen

The State Key Laboratory of High Performance Ceramics and Superfine Microstructure,
Shanghai Institute of Ceramics, Chinese Academy of Sciences, Shanghai 200050, People's Republic of China

(Received 25 August 1993; revised version received 26 November 1993; accepted 14 December 1993)

Abstract

R–α'–β'-Sialon (R = Sm, Gd, Dy, Y and Yb) compositions with a nominal 1 : 1 weight ratio of α' and β' have been prepared. Nearly fully dense α'–β'-sialon materials were obtained by pressureless sintering at 1800°C. The phase distribution was determined by both X-ray diffraction and image analysis of SEM micrographs. The atomic number of rare earth elements has a significant effect on the phase distribution. With increasing atomic number the ratio α'/(α'+ β') increases and the amount of liquid phase decreases. The influences of rare earth elements on the microstructure and mechanical properties were also studied.

Es wurden R–α'–β'-Sialon-Komposite (R = Sm, Gd, Dy, Y und Yb) mit einem nominellen Gewichtsverhältnis von α' and β' von 1 : 1 hergestellt. Durch druckloses Sintern bei 1800°C konnte nahezu die volle Dichte der α'–β'-Sialone erreicht werden. Die Bestimmung der Phasenverteilung erfolgte mit Hilfe von Röntgenbeugung und Bildanalyse der SEM-Aufnahmen. Die Atomzahl der seltenen Erdelemente hat einen bedeutenden Einfluß auf die Phasenverteilung. Mit zunehmender Atomzahl nimmt das Verhältnis α'/(α'+β') zu und die Menge an flüssiger Phase ab. Weiterhin wurde der Einfluß der seltenen Erdelemente auf das Gefüge und die mechanischen Eigenschaften untersucht.

On a préparé des sialons R–α'–β' (R = Sm, Gd, Dy, Y et Yb), où les phases α' et β' sont en rapport massique de 1 : 1. On a obtenu des sialons α'–β' presque totalement denses par frittage naturel à 1800°C. On a déterminé la distribution des phases par diffraction X et analyse des micrographies obtenues au MEB. Le rapport α'/α'+β' croît avec le numéro atomique, alors que la quantité de phase liquide diminue. On a également étudié l'influence des terres rares sur la microstructure et les propriétés mécaniques.

1 Introduction

Si_3N_4-based ceramics are promising materials for high temperature engineering applications.[1–3] Oxide additives are usually used to promote densification by forming a liquid phase with the SiO_2 on the surface of Si_3N_4 powder. The liquid phase, however, remains as glassy phase at grain boundaries after cooling and usually causes deterioration of the high temperature properties of the materials. In order to alleviate the problem, one effective approach is to reduce the amount of intergranular phase by forming a transient liquid phase. Sialon ceramics provide the possibility to produce a transient liquid phase, especially α'-sialon. This is because α-Si_3N_4 structure contains two large isolated interstices where some large metal ions can be accommodated to form α'-sialon. The general formula of α'-sialon is represented as $M_xSi_{12(m+n)}Al_{m+n}O_nN_{16-n}$, where m(Si–N) are substituted by m(Al–N), n(Si–N) by n(Al–O), and the valency discrepancy introduced is compensated by metal ion M. The elements M which have been reported to form α'-sialon are Li, Ca, Mg, Y and R (Nd, Sm, Gd, Dy, Er and Yb).[4–6] The advantage of multiphase α'–β'-sialon over single-phase sialon materials is that the mechanical properties can be tailored, because they can combine high fracture strength of β'-sialon with good hardness of a α'-sialon. Multiphase ceramics can also take an advantage from tailored microstructures, for example, equiaxed α'-sialon grains can be mated with elongated β'-sialon grains to form a toughened texture. On the other hand, α'–β'-sialon compositions are easier to

Journal of the European Ceramic Society 0955-2219/94/$7.00

densify than α'-sialon compositions alone because the former combinations have slightly lower nitrogen contents. Therefore, more attention has recently being focused on α'–β'-sialon materials.[7]

The phase relationships in the Y–Si–Al–O–N system have been reported.[8] On the Si_3N_4–Al_2O_3: AlN—YN : 3AlN plane there exists a α'–β' two-phase region. The boundary of α'-sialon region facing β'–sialon extends from m = 1.3, n = 0 to m = 1, n = 1.7 and the β'-sialon region compatible with α'-sialon is restricted from $\beta_0(Z = 0)$ to $\beta_{10}(Z = 0.8)$. The boundaries of R–α'–β'-sialon have not been determined. However, Huang *et al.*[6] reported that the solubilities of the rare earth ions in α'-sialon with the compositions along the line Si_3N_4–R_2O_3 : 9AlN increase, while the ionic radius of rare earth ions gets smaller, and for Yb ion the limit of solubility has a value of x_{max} = 1.0.

The present work reports the densification behaviour, phase distribution, microstructural features and some mechanical properties of the R–α'–β'-sialon (R = Sm, Gd, Dy, Y and Yb).

2 Experimental

The starting powders used were Si_3N_4 (laboratory made, 1.5 wt % O), AlN (laboratory made, 1.5wt %O), Al_2O_3 (99.95%) and rare earth oxides (Sm_2O_3, Gd_2O_3, Dy_2O_3, Y_2O_3 and Yb_2O_3, all 99.9%). The R–α'–β'-sialon compositions containing 50 wt% β'—sialon ($Si_{5.2}Al_{0.8}O_{0.8}N_{7.2}$) and 50 wt % α'-sialon ($R_{0.33}Si_{9.3}Al_{2.7}O_{1.7}N_{14.3}$, R = Sm, Gd, Dy, Y and Yb), as listed in Table 1, were prepared. The oxygen contents of the silicon nitride and the aluminium nitride powders were taken into account in computing the composition. The mixtures of powders were milled in absolute alcohol for 24h in an alumina jar using silicon nitride media. After drying, the powder mixtures were die-pressed into test bars under 20MPa, and then cold isostatically pressed under a pressure of 200MPa. The pressed compacts were embedded in a protective powder bed (Si_3N_4 + AlN + BN) in a graphite crucible, and sintered at 1800°C for 2.5 h under flowing nitrogen.

Table 1. Weight percentages of starting materials

Rare earth	*Si_3N_4*	*AlN*	*Al_2O_3*	*Sm_2O_3*	*Gd_2O_3*	*Dy_2O_3*	*Y_2O_3*	*Yb_2O_3*
Sm	79.100	10.505	5.099	4.750				
Gd	78.967	10.477	5.091		4.920			
Dy	78.866	10.456	5.086			5.047		
Y	80.332	10.762	5.168				3.183	
Yb	78.666	10.414	5.074					5.303

Bulk density of the specimens was determined using the Archimedes principle. The Vickers hardness (H_V10) and indentation fracture toughness K_{IC} were measured by using a Vickers diamond indenter under 10 kg.[9] Phase distributions were determined by both X-ray diffraction technique (for crystalline phases) and image analysis of SEM micrographs (back-scattering mode). A Kontron IBAS KAT386 image processing system on-line with the Cambridge 360 was used for image analysis. For each sample five photographs (×3000) were selected to be treated. Microstructure was also observed by scanning microscopy.

3 Results and Discussion

3.1 Densification behaviour

All the α'–β'-sialon compositions studied have a weight loss less than 2 wt % after sintering at 1800°C and the bulk density can exceed 98% of the theoretical value (Fig. 1). The Sm–α'–β'-sialon composition has the highest relative density (99%) and the Gd– and Dy–sialon compositions have slightly lower values. The dependence of atomic number (Z value) of rare earth elements on the densification behaviour is not very obvious. The amount of liquid phase and its viscosity are the main elements to effect the densification process. However, knowledge of the liquid-phase formation in the R–Si–Al–O–N system is too scarce to be used to understand its effect on the densification behaviour. Recent work on the phase relationships in the Sm–Si–Al–O–N system indicates there exists a rather big liquid-phase region with a nitrogen content up to 40 equivalent %. The phase distribution determined in the present work also indicates that the Sm–sialon composition contains the highest content of liquid phase, as described later. Therefore, the relatively larger amount of liquid phase in the Sm-sialon composition could be the main reason for attaining a higher density.

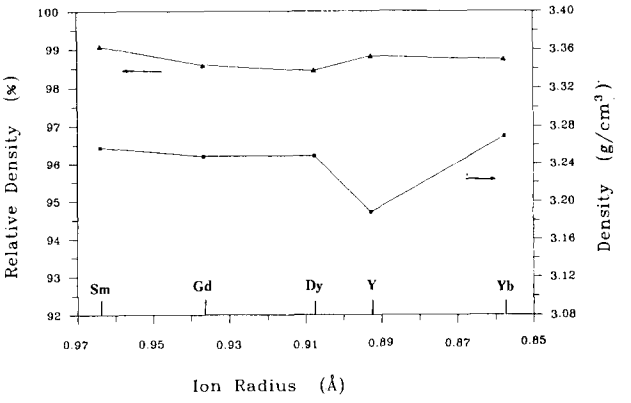

Fig. 1. Effects of different rare earth elements on the density of R–α'–β'-sialons.

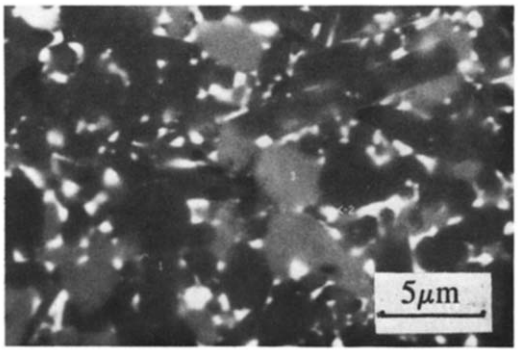

Fig. 2. SEM photograph (back-scattering mode) of Y–α'–β'-sialon.

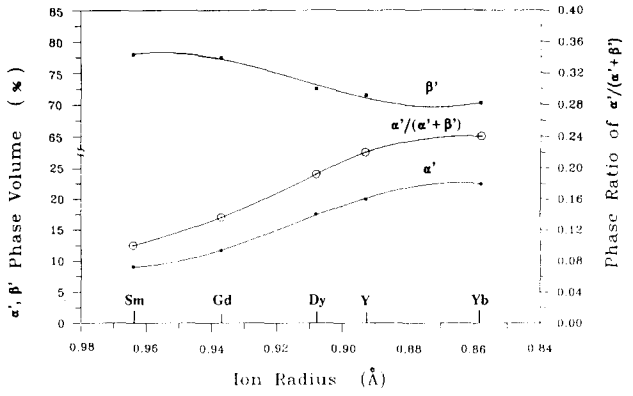

Fig. 3. Volume percentage of α'-, β'-phase and the α'/(α'+β') ratio in R–α'–β'-sialons.

3.2 Phase distribution

XRD analysis shows that the only crystalline phases in the samples are α'-sialon and β'-sialon, and the intergranular phase exists in the glassy state. As is known, all rare earth ions smaller than Nd^{3+} can enter the α'-sialon structure, whereas the β'-sialon does not incorporate any such large cations. Based on the detectable contrast shown by different phases—α', β' and liquid phase—under back-scattering mode, their volume fractions can be determined. In the present case, the scattering intensities are directly relevant to the concentration of the rare earth ions in each phase. Under the experimental conditions used, the concentration of the rare ions in the glassy phase is higher than that in the α'-sialon phase. Figure 2 is a typical micrograph of the R–α'–β'-sialons under back-scattering mode.

The largest amount of dark grey grains are the β'-sialon phase, the bright areas are the glassy phase and α'-sialon grains are those with the light grey shade. The phase distributions in as-sintered specimens obtained by both X-ray diffraction and image analysis of SEM micrographs are listed in Table 2 and are also represented in Fig. 3 and 4. As expected, there is no big difference between these two approaches. As shown in Table 2, the phase ratio α'/(α'+β') in the as-sintered specimens is lower than the expected value of 0.5 and, with increasing Z value of the rare earth elements, the α'/(α'+β') ratio increases. This phenomenon is similar to previous work[10] and that observed by Ekström *et al.*[11] Obviously, smaller rare earth cations are more easily accommodated in the α'-sialon structure, leaving less in the liquid phase at the grain boundaries. The Sm–sialon composition has the lowest content, 7%.

Table 2. Phase contents (vol.%) of different sialons obtained from XRD analysis and image analysis

Samples	*Sm–Sialon*	*Gd–Sialon*	*Dy–Sialon*	*Y–Sialon*	*Yb–Sialon*
XRD analysis					
α'/(α' + β')	0.06	0.11	0.16	0.19	0.21
Image analysis					
α'/(α' + β')	0.10	0.13	0.19	0.22	0.24
Glassy phase (vol.%)	12.90	10.70	10.00	8.3	7.1

3.3 Microstructure

The typical microstructure of the R–α'–β'-sialon compositions (R = Sm, Gd, Dy, Y and Yb) are shown in Fig. 5. the influence of rare earth elements on their microstructure is detectable. The microstructures of Sm– and Gd–sialons are composed of finer grains with relatively large amount of intergranular glassy phase. With an increasing atomic number of the rare earth elements, the crystallites grow into larger grains for reasons not yet very clear. Dy– and Y–sialons seem to have rather perfect microstructures which are composed of elongated grains and equiaxed grains with smaller amounts of glassy phase. A certain amount of liquid phase is a necessary environment for crystallites to grow into anisotropic and faceted morphology. The thicker β' grains with lower aspect ratio in the Yb–sialon compositions may be attributed to the characteristics and the amount of the liquid phase. Further study on the kinetics of β'-phase growth is needed.

3.4 Mechanical properties

The hardness and fracture toughness of the R–α'–β'-sialon compositions are represented in

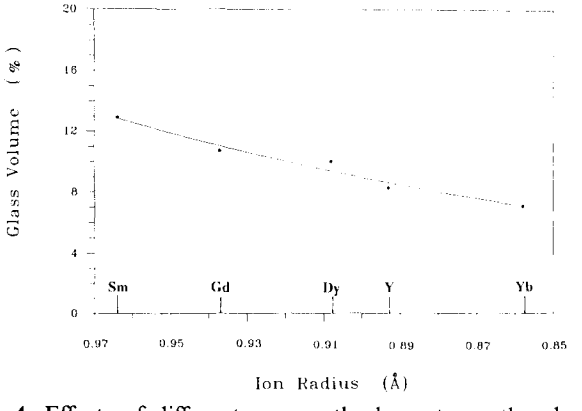

Fig. 4. Effects of different rare earth elements on the glassy phase volume in R–α'–β'-sialons.

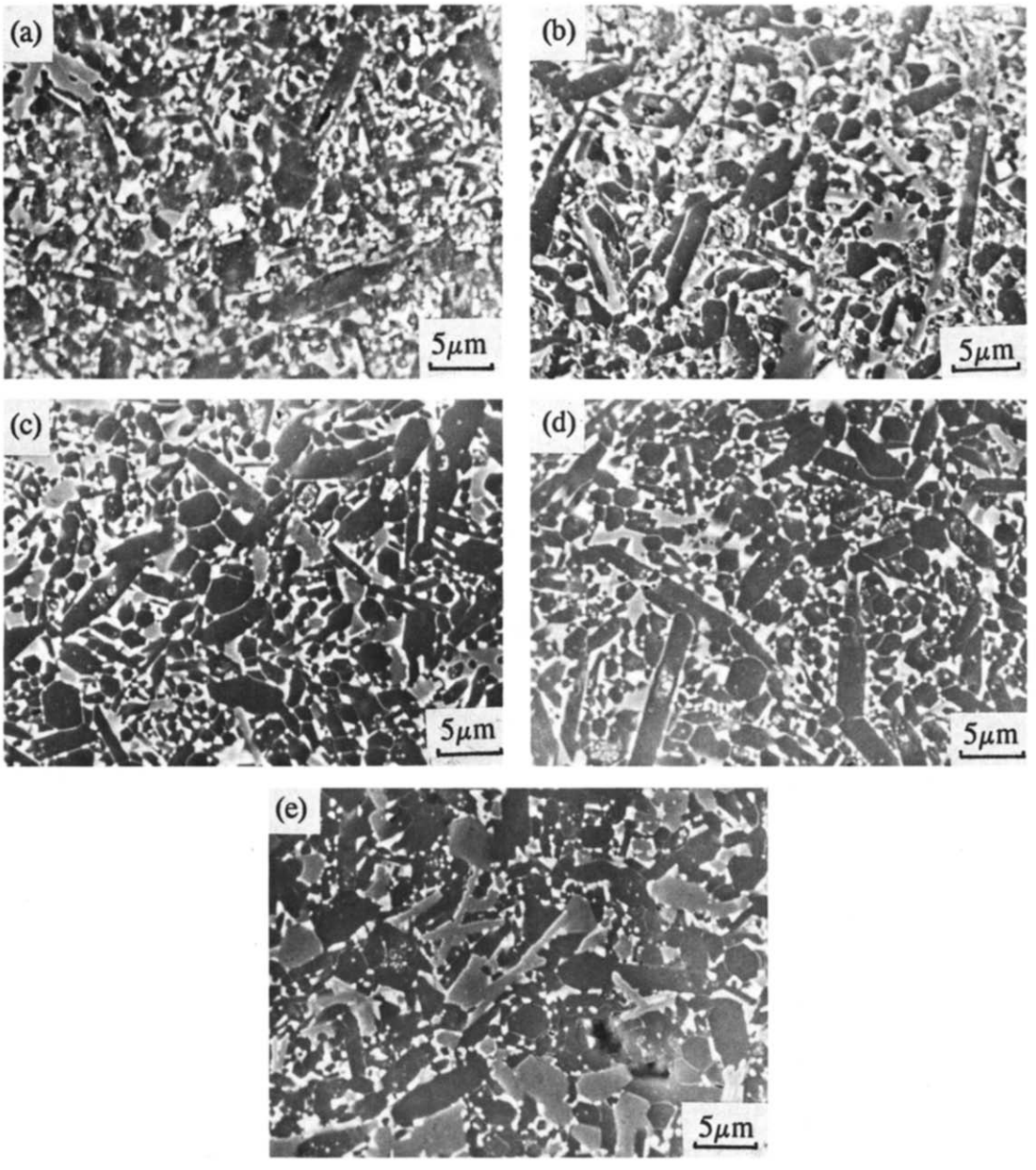

Fig. 5. Scanning electron micrographs of R–α'–β'-sialon materials. The rare earth elements used are: (a) Sm, (b) Gd, (c) Dy, (d) Y, (e) Yb.

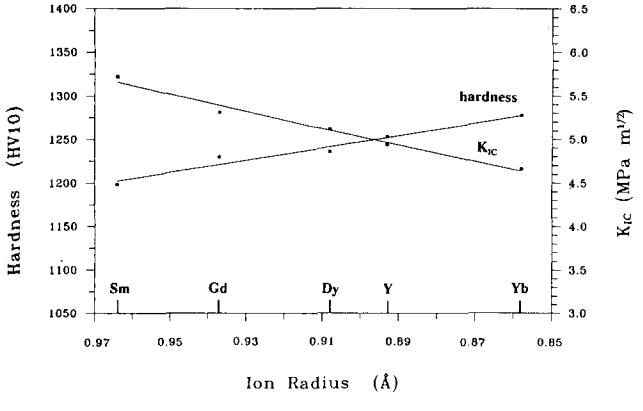

Fig. 6. Vickers hardness (H_V10) and identation fracture toughness (K_{IC}) of α'–β'-sialon as a function of the ionic radius of rare earth elements.

Fig. 6. Apparently, the dependence of the mechanical properties on Z value of rare earth elements is closely related to the phase compositions, because α'-sialon possesses a significantly higher hardness and β'-sialon has a reasonably higher fracture toughness. In the Sm–sialon composition, the lower ratio of $\alpha'/(\alpha'+\beta')$ results in a higher fracture toughness and a lower hardness. The Yb–sialon composition, with the highest ratio of $\alpha'/(\alpha'+\beta')$ in the series, has the highest hardness and the lowest fracture toughness. Beside the phase compositions, the relative density and the microstructure must have some influence on the properties. However, in the present case, the main factor to influence the hardness and fracture toughness seems to be the $\alpha'/(\alpha'+\beta')$ phase ratio in the compositions.

4 Conclusions

(1) α'–β'-Sialon compositions using rare earth oxides Sm_2O_3, Gb_2O_3, Dy_2O_3, Y_2O_3 and Yb_2O_3 as 'modifying cation' resources can be sintered above 98% theoretical density by pressureless sintering.

(2) The ionic size of rare earth elements has a significant effect on the phase compositions. With an increasing atomic number of the rare earth elements, the phase ratio $\alpha'/(\alpha'+\beta')$ increases from 0.1 to 0.24 and the fraction of liquid phase formed under the present sintering conditions decreases from 13% to 7%.

(3) The mechanical properties of R–α'–β'-sialon ceramics are relevant to the phase compositions. The Sm–sialon compositions, with a lower ratio of $\alpha'(\alpha'+\beta')$, has a higher fracture toughness, while the Yb–sialon composition, with a higher value of $\alpha'/(\alpha'+\beta')$ ratio, gives a higher hardness.

References

1. Jack, K. H., Sialon tool materials. *Metal Technol.*, **9** (1982) 297–301.
2. Richerson, D. W., Evolution in the US of ceramic technology for turbine engines. *Amer. Ceram. Soc. Bull.*, **64** (1985) 282–6.
3. Yamaguchi, J., Isuzu's state-of-the art diesel engine. *Auto. Engin.*, **96**(3) (1988) 78–9.
4. Park, H. K., Thompson, D. P. & Jack, K. H., α'-Sialon ceramics. *Sci. Ceram.*, **10** (1980) 251–6.
5. Huang, Z. K., Greil, P. & Petzow, G., Formation of α-Si_3N_4 solid solutions in the system Si_3N_4–AlN–Y_2O_3. *J. Amer. Ceram. Soc.*, **66** (1983) C96–C97.
6. Huang, Z. K., Tien T. Y. & Yen, T. S., Subsolidus phase relationships in Si_3N_4–AlN–rare-earth oxide systems. *J. Am. Ceram. Soc.*, **69** (1986) C241–C242.
7. Ekstrom, T. & Nygren, M., SiAlON ceramics. *J. Amer. Ceram. Soc.*, **75** (1992) 259–76.
8. Sun, W. Y. Tien, T. Y. & Yen, T. S., Solubility limits of α'-SiAlON solid solutions in the system Si,Al,Y/N,O. *J. Amer. Ceram. Soc.*, **74** (1991) 2547–50.
9. Anstis, G. R., Chantikul, P., Lawn, B. R. & Marshall, D. B., A critical evaluation of indentation techniques for measuring fracture toughness. *J. Amer. Ceram. Soc.*, **64** (1981) 533–8.
10. Wang, P. L., Sun, W. Y. & Yen, T. S., Formation and densification of *R*–α'–β'–SiAlONs (*R* = Nd, Sm, Gd, Er and Yb). In *Silicon Nitride Ceramics, Scientific and Technological Advances*, ed. I. W. Chen *et al.* Materials Research Society, Pittsburgh, PA, 1993, pp. 387–91.
11. Ekström, T., Jansson, K., Olsson, P. O. & Persson, J., Formation of an Y/Ce doped α-sialon phase. *J. Eur. Ceram. Soc.*, **8** (1991) 3–9.